Improper Gaussian Signaling for Broadcast Interference Networks

Nasir, A. A., Tuan, H. D., Duong, Q., & Poor, H. V. (2019). Improper Gaussian Signaling for Broadcast Interference Networks. *IEEE Signal processing Letters*, *26*(6), 808 - 812. https://doi.org/10.1109/LSP.2019.2905959

Published in:
IEEE Signal processing Letters

Document Version:
Peer reviewed version

Improper Gaussian Signaling for Broadcast Interference Networks

A. A. Nasir, H. D. Tuan, T. Q. Duong and H. V. Poor

***Abstract*—The use of improper Gaussian signaling (IGS) helps to improve the achievable rate of interference-limited wireless multiple-input-multiple-output (MIMO) communication networks. For a general multi-user multi-cell network, which suffers both intra-cell and inter-cell interference, this letter considers the design of signals' augmented covariance matrices to maximize the users' minimum rate subject to transmit power constraint. This is a nonconvex matrix optimization problem, which cannot be solved by popular techniques such as weighted minimum mean square error minimization or alternating optimization. This letter proposes a path-following algorithm, which iterates a sequence of improved feasible points for its computation. The provided simulation results for three cells serving 18 users show that the use of IGS offers a much better max-min rate compared to that achieved by the conventional proper Gaussian signaling. Its extension to the problem of maximizing the energy efficiency in IGS is also considered.**

***Index Terms*—Multi-user interference system, multi-input multi-output (MIMO), improper Gaussian signaling (IGS), augmented covariance matrix, nonconvex optimization, quality-of-service (QoS).**

I. Introduction

The massive data demand in today's wireless networks triggers sharing wireless spectrum among users. This may result in intra-cell and inter-cell interference, which can be managed with the help of advanced signal processing techniques. Recently, it has been shown that improper Gaussian signaling (IGS) can improve the achievable rate in interference-limited scenarios [1], [2]. In contrast to conventional proper Gaussian signaling (PGS), under which the transmit signals are proper Gaussian and are fully characterized by their covariance matrix, IGS relaxes the Gaussian properness to augment the degree of freedom. Hence, improper Gaussian signals are characterized by the so called augmented covariance matrices, which are composed from both covariance and pseudo-covariance matrices [3]. As such, improper Gaussian signals can be generated from proper Gaussian information bearing sources through widely linear precoding [3].

The superiority of IGS over PGS in terms of achievable rates in single-input single-output (SISO) interference channels (ICs) has been analyzed in [4]–[7]. Considering multiple-input multiple-output (MIMO) ICs, the dominance of IGS over PGS has been studied in terms of degree of freedom [1], [2], [8], in terms of Qos feasibility [9], or in terms of achievable rates [10]. However, the degree of freedom is an appropriate metric only under very high signal-to-noise ratios. In [10], the authors addressed the design problem of widely linear precoding to maximize the weighted sum-rate.

This letter considers IGS for multi-user multi-cell MIMO interference networks, where the base stations (BSs) broadcast signals to their users. Different from the existing works, we are interested in designing of signals' augmented covariance matrices to maximize the users' minimum rate subject to transmit power constraint. This is a computationally challenging nonconvex optimization problem. On one hand, the augmented covariance matrices are no longer structure-free and thus cannot be analytically factorized into outer products of structure-free precoder matrices for applying the popular techniques such as weighted minimum mean square error (WMMSE) [11], [12] to computational solution. On the other hand, alternating optimization for broadcast channels in multi-user multi-cell MIMO interference networks is not computationally tractable either because each alternating iteration still involves a nonconvex matrix optimization problem. Nevertheless, we propose a path-following algorithm, which improves feasible points after each iteration and converges at least to a locally optimal solution to address this problem. In addition, we extend our algorithm to solve an interesting problem of maximizing the energy efficiency of the network. We compare the performance of the proposed algorithm with the ones that solve the said problems under PGS. Our simulation results show that the use of IGS offers a much better max-min rate and energy efficiency compared to that achieved by the conventional PGS.

The rest of the paper is organized as follows. Section II is devoted to the problem statement and analysis of computational difficulties. A path-following algorithm for computational solution is proposed in Section III, which is supported by simulations conducted in Section III. The conclusions are given in Section IV.

Notation: I_n is the identity matrix of size $n \times n$. X^H, X^T, and X^* are the Hermitian transpose, normal transpose, and conjugate of the matrix X, respectively. The inner product $\langle X, Y\rangle$ of the matrices X and Y is defined as trace$(X^H Y)$. Denote by $\langle A\rangle$ the trace of the matrix A, and by $|A|$ its determinant. $\|\cdot\|$ stands for matrix's Frobenius norm or vector's Euclidean norm. $\mathbb{C}$ is the set of all complex numbers. $\mathbb{E}\{\cdot\}$ denotes the expectation operator. Only design variables are boldface typed. $\mathbf{X} \succeq 0$ means that the matrix $\mathbf{X}$ is positive definite.

A. A. Nasir is with the Department of Electrical Engineering, King Fahd University of Petroleum and Minerals (KFUPM), Dhahran, Saudi Arabia (email: anasir@kfupm.edu.sa).

Hoang Duong Tuan is with the School of Electrical and Data Engineering, University of Technology Sydney, Broadway, NSW 2007, Australia (email: Tuan.Hoang@uts.edu.au).

Trung Q. Duong is with Queen's University Belfast, Belfast BT7 1NN, UK (email: trung.q.duong@qub.ac.uk).

H. Vincent Poor is with the Department of Electrical Engineering, Princeton University, Princeton, NJ 08544, USA (-mail: poor@princeton.edu)

II. System Model and Problem Formulation

Consider the downlink of a multiuser multi-cell wireless communication system which consists of N cells, where the base station (BS) of each cell is equipped with N_t antennas to serve K users (also called user equipments, or UEs) within its cell. Each UE is equipped with $N_r \geq 1$ antennas. Let us define $\mathcal{I} := \{1, 2, \ldots, N\}$ and $\mathcal{J} := \{1, 2, \ldots, K\}$. The jth UE in the ith cell is referred to as UE (i, j). Let $H_{m,i,j} \in \mathbb{C}^{N_r \times N_t}$ be the MIMO channel matrix from the BS m to UE (i, j). Accordingly, $H_{i,i,j}$ and $H_{m,i,j}$ for $m \neq i$ are the direct and interfering channels with respect to UE (i, j). The complex baseband signal $y_{i,j} \in \mathbb{C}^{N_r}$ received by the UE (i, j) is given by

$$\begin{aligned} y_{i,j} &= \sum_{m=1}^{N} H_{m,i,j} x_m + n_{i,j} \\ &= H_{i,i,j} x_{i,j} + z_{i,j} + n_{i,j}, \end{aligned} \tag{1}$$

where

- $x_m \in \mathbb{C}^{N_t}$ is the broadcast signal from the BS m, which is a superposition of the signals $x_{m,k} \in \mathbb{C}^{N_t}$ intended for users (m, k): $x_m = \sum_{k=1}^{K} x_{m,k}$;
- $H_{i,i,j} x_{i,j}$ is the signal of interest;
- $z_{i,j} \triangleq \sum_{(m,k) \in \mathcal{I} \setminus \{(i,j)\}} H_{m,i,j} x_{m,k}$ is the interfering signal;
- $n_{i,j} \in \mathbb{C}^{N_r}$ is the background noise and its entries represent i.i.d. Gaussian noise samples with zero-mean and variances σ^2.

We are interested in IGS, under which each $x_{m,k}$ is complex Gaussian (not necessarily symmetric) with zero means and thus is characterized by the so called augmented covariance $\mathbf{C}^A_{m,k}$ defined as [13]

$$\mathbf{C}^A_{m,k} \triangleq \mathbb{E}\left\{ \begin{bmatrix} x_{m,k} \\ x^*_{m,k} \end{bmatrix} \begin{bmatrix} x_{m,k} \\ x^*_{m,k} \end{bmatrix}^H \right\} = \begin{bmatrix} \mathbf{C}_{m,k} & \widetilde{\mathbf{C}}_{m,k} \\ \widetilde{\mathbf{C}}^*_{m,k} & \mathbf{C}^*_{m,k} \end{bmatrix}, \tag{2}$$

which is the covariance of the augmented signal $\begin{bmatrix} x_{m,k} \\ x^*_{m,k} \end{bmatrix}$. In the expression (2), $\mathbf{C}_{m,k} \triangleq \mathbb{E}\{x_{m,m} x^H_{m,k}\}$ and $\widetilde{\mathbf{C}}_{m,k} \triangleq \mathbb{E}\{x_{m,k} x^T_{m,k}\}$ respectively are the covariance matrix and pseudo-covariance matrix of $x_{m,k}$. In fact, $\mathbf{C}_{m,k}$ and $\widetilde{\mathbf{C}}_{m,k}$ are qualified as the covariance and pseudo-covariance matrices of $x_{m,k}$ if and only if they satisfy the following semi-definite constraint to make $\mathbf{C}^A_{m,k}$ positive-definite:

$$\begin{bmatrix} \mathbf{C}_{m,k} & \widetilde{\mathbf{C}}_{m,k} \\ \widetilde{\mathbf{C}}^*_{m,k} & \mathbf{C}^*_{m,k} \end{bmatrix} \succeq 0, (m, k) \in \mathcal{I} \times \mathcal{J}. \tag{3}$$

We express the augmented signal of interest

$$\begin{bmatrix} H_{i,i,j} x_{i,j} \\ (H_{i,i,j} x_{i,j})^* \end{bmatrix} = \begin{bmatrix} H_{i,i,j} & 0_{N_r \times N_t} \\ 0_{N_r \times N_t} & H^*_{i,i,j} \end{bmatrix} \begin{bmatrix} x_{ij} \\ x^*_{ij} \end{bmatrix}$$

to derive the augmented covariance of $H_{i,i,j} x_{i,j}$ as the following congruent transformation of $\mathbf{C}^A_{i,j}$:

$$\begin{aligned} \Lambda_{i,j}(\mathbf{C}^A_{i,j}) \triangleq \\ \begin{bmatrix} H_{i,i,j} & 0_{N_r \times N_t} \\ 0_{N_r \times N_t} & H^*_{i,i,j} \end{bmatrix} \mathbf{C}^A_{i,j} \begin{bmatrix} H_{i,i,j} & 0_{N_r \times N_t} \\ 0_{N_r \times N_t} & H^*_{i,i,j} \end{bmatrix}^H \end{aligned} \tag{4}$$

which is a linear mapping of $\mathbf{C}^A_{i,j}$.

Analogously, we express the augmented interfering signal

$$\begin{bmatrix} z_{i,j} \\ z^*_{i,j} \end{bmatrix} = \sum_{(m,k) \in \mathcal{I} \setminus \{(i,j)\}} \begin{bmatrix} H_{m,i,j} & 0_{N_r \times N_t} \\ 0_{N_r \times N_t} & H^*_{m,i,j} \end{bmatrix} \begin{bmatrix} x_{m,k} \\ x^*_{m,k} \end{bmatrix}$$

to derive the augmented covariance matrix of $z_{i,j}$ as

$$\begin{aligned} \mathcal{M}_{i,j}(\mathbf{C}^A) &= \sum_{(m,k) \in \mathcal{J} \setminus \{(i,j)\}} \begin{bmatrix} H_{m,i,j} & 0_{N_r \times N_t} \\ 0_{N_r \times N_t} & H^*_{m,i,j} \end{bmatrix} \mathbf{C}^A_{m,k} \\ &\quad \times \begin{bmatrix} H_{m,i,j} & 0_{N_r \times N_t} \\ 0_{N_r \times N_t} & H^*_{m,i,j} \end{bmatrix}^H \end{aligned} \tag{5}$$

which is obviously a linear mapping of $\mathbf{C}^A \triangleq (\mathbf{C}^A_{i,j})_{(i,j) \in \mathcal{I} \times \mathcal{J}}$.

The rate (in nats) at UE (i, j) is then defined by [14]

$$\begin{aligned} r_{i,j}(\mathbf{C}^A) \triangleq \\ \frac{1}{2} \ln \left| I_{2N_r} + \Lambda_{i,j}(\mathbf{C}^A_{i,j}) \left(\mathcal{M}_{i,j}(\mathbf{C}^A) + \sigma^2 I_{2N_r} \right)^{-1} \right|. \end{aligned} \tag{6}$$

Accordingly, the design of IGS to maximize the users' minimum rate is formulated as the following max-min rate optimization problem:

$$\max_{\mathbf{C}^A} \ \Psi(\mathbf{C}^A) \triangleq \min_{(i,j) \in \mathcal{I} \times \mathcal{J}} r_{i,j}(\mathbf{C}^A) \quad \text{s.t.} \quad (3), \tag{7a}$$

$$\sum_{j=1}^{K} \langle \mathbf{C}_{i,j} \rangle \leq P_i, i = 1, \ldots, N, \tag{7b}$$

where P_i is the maximum power budget at the BS i. The objective function in (7) is not only non-concave but also non-smooth, making it computationally difficult. Due to the structure of the augmented covariance $\mathbf{C}^A_{m,k}$ in (2), it is impossible to analytically factorize it into outer products of precoder matrices so the popular WMMSE [11], [12] is not applicable. It is also obvious that the objective function in (7) remains nonconcave in $\mathbf{C}^A_i \triangleq (\mathbf{C}^A_{i,1}, \ldots, \mathbf{C}^A_{i,K})$ with other $\mathbf{C}^A_\ell \triangleq (\mathbf{C}^A_{\ell,1}, \ldots, \mathbf{C}^A_{\ell,K})$, $\ell \neq i$ held fixed, so alternating optimization, which is used in [10] for ICs ($K = 1$), is not workable. Furthermore, although each $r_{i,j}(\mathbf{C}^A)$ is the d.c. (difference of two concave functions) function [15]

$$\begin{aligned} \tfrac{1}{2} \ln \left| (1 + \sigma^2) I_{2N_r} + \Lambda_{i,j}(\mathbf{C}^A_{i,j}) + \mathcal{M}_{i,j}(\mathbf{C}^A) \right| \\ - \tfrac{1}{2} \ln \left| \mathcal{M}_{i,j}(\mathbf{C}^A) + \sigma^2 I_{2N_r} \right|, \end{aligned}$$

and so (7) can be addressed by the d.c. iterations [16], which however are not efficient by involving optimization of logarithm determinant functions at each iteration with no known solver of polynomial time complexity.

III. Proposed Algorithm

In this section, we propose a path following algorithm to solve the max-min rate optimization problem (7). First, let us recall the following result [17].

Proposition 1: For $\mathbf{X} \succeq 0$, $\bar{X} \succeq 0$, $\mathbf{Y} \succeq 0$ and $\bar{Y} \succeq 0$ of sizes $(2N_r) \times (2N_r)$, it is true that

$$\begin{aligned} \ln |I_{2N_r} + \mathbf{X}(\mathbf{Y} + \sigma^2 I_{2N_r})^{-1}| \geq \\ a - \langle \bar{X} + \bar{Y} + \sigma^2 I_{2N_r}, (\mathbf{X} + \mathbf{Y} + \sigma^2 I_{2N_r})^{-1} \rangle \\ - \langle (\bar{Y} + \sigma^2 I_{2N_r})^{-1}, \mathbf{Y} \rangle \end{aligned} \tag{8}$$

with $a = \ln |I_{2N_r} + \bar{X}(\bar{Y} + \sigma^2 I_{2N_r})^{-1}| + 4N_r - \sigma^2 \langle (\bar{Y} + \sigma^2 I_{2N_r})^{-1} \rangle$. The function defined by (8) is concave in $(\mathbf{X}, \mathbf{Y})$

Algorithm 1 IGS-based Proposed Algorithm to solve Max-min Rate Optimization Problem (7).

Initialization: Set $\kappa := 0$ and a feasible point $C^{A,(0)}$ using random covariance $C_{i,j}^{(0)}$ and pseudo-covariance matrices $\widetilde{C}_{i,j}^{(0)}$, $\forall\ (i,j) \in \mathcal{I} \times \mathcal{J}$, satisfying the power constraint (3).

1: **repeat**
2: Solve the convex optimization problem (10) to obtain the optimal solution $C^{A,(\kappa+1)}$.
3: Set $\kappa := \kappa + 1$.
4: **until** Convergence of the objective in (7).

because its second term is a concave function [18], while its third term is obviously a linear function. □

Now, let $C^{A,(\kappa)} \triangleq (C_{i,j}^{A,(\kappa)})_{(i,j)\in\mathcal{I}\times\mathcal{J}}$ be a feasible point for (7) that is found at the $(\kappa-1)$th iteration, where

$$C_{i,j}^{A,(\kappa)} = \begin{bmatrix} C_{i,j}^{(\kappa)} & \widetilde{C}_{i,j}^{(\kappa)} \\ \left(\widetilde{C}_{i,j}^{(\kappa)}\right)^* & \left(C_{i,j}^{(\kappa)}\right)^* \end{bmatrix}.$$

With regard to the function $r_{i,j}(\mathbf{C}^A)$ in (7a), applying inequality (8) for $\mathbf{X} = \Lambda_{i,j}(\mathbf{C}_{i,j}^A)$, $\mathbf{Y} = \mathcal{M}_{i,j}(\mathbf{C}^A)$ and $\bar{X} = \Lambda_{i,j}(C_{i,j}^{A,(\kappa)})$, $\bar{Y} = \mathcal{M}_{i,j}(C^{A,(\kappa)})$ yields the following lower concave function approximation

$$\begin{aligned} r_{i,j}(\mathbf{C}^A) \quad &\geq \\ a^{(\kappa)} - \Big\langle \Lambda_{i,j}(C_{i,j}^{A,(\kappa)}) &+ \mathcal{M}_{i,j}(C^{A,(\kappa)}) \\ +\sigma^2 I_{2N_r}, (\Lambda_{i,j}(\mathbf{C}_{i,j}^A) &+ \mathcal{M}_{i,j}(\mathbf{C}^A) + \sigma^2 I_{2N_r})^{-1} \Big\rangle \\ - \Big\langle (\mathcal{M}_{i,j}(C^{A,(\kappa)}) &+ \sigma^2 I_{2N_r})^{-1}, \mathcal{M}_{i,j}(\mathbf{C}^A) \Big\rangle \quad \triangleq \\ & r_{i,j}^{(\kappa)}(\mathbf{C}^A), \end{aligned} \tag{9}$$

with $a^{(\kappa)} = \ln \Big| I_{2N_r} + \Lambda_{i,j}(C_{i,j}^{A,(\kappa)})(\mathcal{M}_{i,j}(C^{A,(\kappa)}) + \sigma^2 I_{2N_r})^{-1} \Big| + 4N_r - \sigma^2 \left\langle (\mathcal{M}_{i,j}(C^{A,(\kappa)}) + \sigma^2 I_{2N_r})^{-1} \right\rangle$.

Thus, at the κ-th iteration, we solve the following convex optimization problem to generate the next iterative feasible point $C^{A,(\kappa+1)}$ for (7):

$$\max_{\mathbf{C}^A} \Psi^{(\kappa)}(\mathbf{C}^A) \triangleq \min_{(i,j)\in\mathcal{I}\times\mathcal{J}} r_{i,j}^{(\kappa)}(\mathbf{C}^A) \quad \text{s.t.} \quad (3), (7b). \tag{10}$$

The computational complexity of this problem is $\mathcal{O}\left((2KNN_t^2)^3 (KN+N)\right)$ [19].

Algorithm 1 outlines the steps to solve the max-min rate problem (7). Note that $\Psi^{(\kappa)}(C^{A,(\kappa+1)}) > \Psi^{(\kappa)}(C^{A,(\kappa)})$ because $C^{A,(\kappa+1)}$ is the optimal solution of (10) while $C^{A,(\kappa)}$ is its feasible point. Therefore, $\Psi(C^{A,(\kappa+1)}) \geq \Psi^{(\kappa)}(C^{A,(\kappa+1)}) > \Psi^{(\kappa)}(C^{A,(\kappa)}) = \Psi(C^{A,(\kappa)})$, where the last equality follows from the equality $r_{i,j}^{(\kappa)}(C^{A,(\kappa)}) = r_{i,j}(C^{A,(\kappa)})$, which is easily checked using the definition (9). Algorithm 1 thus generates a sequence $\{C^{A,(\kappa)}\}$ of improved feasible points for (7). Using similar arguments as in [20], it can be easily shown that Algorithm 1 at least converges to a locally optimal solution of (7), which satisfies the Karush-Kuh-Tucker (KKT) optimality condition. It is noteworthy to point out that the simulation results in [20] show that this type of solution is often globally optimal.

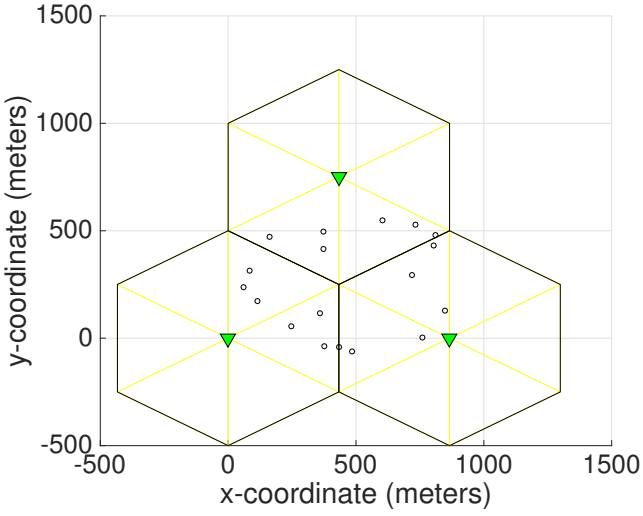

Fig. 1. A multi-cell network setup where triangles at the center of the cells denote the BSs and circles show the users' positions.

Remark. The problem of energy-efficiency maximization under QoS constraints,

$$\max_{\mathbf{C}^A} \sum_{(i,j)\in\mathcal{I}\times\mathcal{J}} r_{i,j}(\mathbf{C}^A)/\varphi(\mathbf{C}^A) \quad \text{s.t.} \quad (3), (7b), \tag{11a}$$

$$r_{i,j}(\mathbf{C}^A) \geq r_{i,j}^{\min}, (i,j) \in \mathcal{I}\times\mathcal{J}, \tag{11b}$$

can be addressed similarly, where $r_{i,j}^{\min}$ is the rate threshold to express the required QoS for UE (i,j) and $\varphi(\mathbf{C}^A) = \sum_{(i,j)\in\mathcal{I}\times\mathcal{J}} \langle \mathbf{C}_{i,j} \rangle + P_{\text{non}}$ is the power consumed by all the BSs, where $P_{\text{non}} = NN_tP_u$ is the non-transmission power and P_u is the per antenna circuit power at the BSs. Initialized by a feasible point $C^{A,(0)}$, which can be located by using Algorithm 1, at the κ-th iteration, we solve the following convex problem instead of (10) to generate the next feasible point $C^{A,(\kappa+1)}$:

$$\max_{\mathbf{C}^A} \Phi^{(\kappa)}(\mathbf{C}^A) \triangleq \sum_{(i,j)\in\mathcal{I}\times\mathcal{J}} r_{i,j}^{(\kappa)}(\mathbf{C}^A) - \theta^{(\kappa)}\varphi(\mathbf{C}^A) \tag{12a}$$

$$\text{s.t.} \quad (3), (7b), r_{i,j}^{(\kappa)}(\mathbf{C}^A) \geq r_{i,j}^{\min}, (i,j) \in \mathcal{I}\times\mathcal{J}, \tag{12b}$$

where $\theta^{(\kappa)} \triangleq \sum_{(i,j)\in\mathcal{I}\times\mathcal{J}} r_{i,j}(C^{A,(\kappa)})/\varphi(C^{A,(\kappa)})$, is the value of the objective function in (11) at $C^{A,(\kappa)}$. Note that $\Phi^{(\kappa)}(C^{A,(\kappa)}) = 0$, so $\Phi^{(\kappa)}(C^{A,(\kappa+1)}) > 0$ at the optimal solution $C^{A,(\kappa+1)}$, which means $\theta^{(\kappa+1)} \triangleq \sum_{(i,j)\in\mathcal{I}\times\mathcal{J}} r_{i,j}(C^{A,(\kappa+1)})/\varphi(C^{A,(\kappa+1)}) > \theta^{(\kappa)}$, i.e. $\{C^{A,(\kappa)}\}$ is a sequence of improved feasible points for (11), which at least converges to a locally optimal solution.

IV. Simulations

As shown in Fig. 1, users are randomly placed in a three-cell network, $N = 3$. Each cell radius is 500 meters. In our simulations, the channel $H_{m,i,j}$ from BS $m \in \mathcal{I}$ to UE (i,j) at a distance of d meters is generated as $H_{m,i,j} = \sqrt{10^{-\sigma_{\text{PL}}/10}}\tilde{H}_{m,i,j}$, where $\tilde{H}_{m,i,j} \in \mathbb{C}^{N_r\times N_t}$ is a normalized Rayleigh fading MIMO channel matrix, $\sigma_{\text{PL}} = 38.46 + 10\beta\log_{10}(d)$ is the path-loss in dB, where the loss factor 38.46 is the free space path loss at a reference distance of 1 meters at carrier frequency of 2 GHz, and $\beta = 3.1$ is the path-loss exponent [21]. For simplicity,

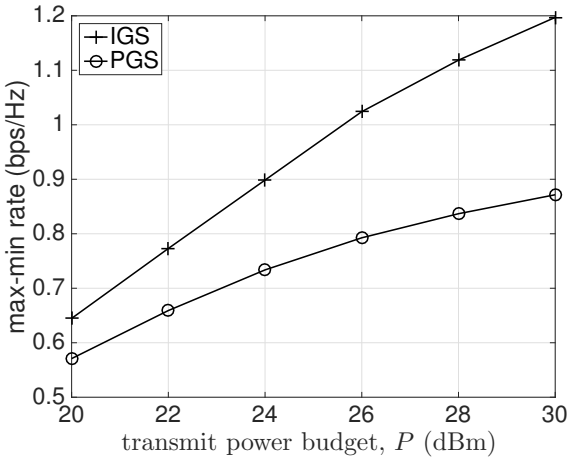

Fig. 2. Optimized max-min user rate for varying values of transmit power budget, P.

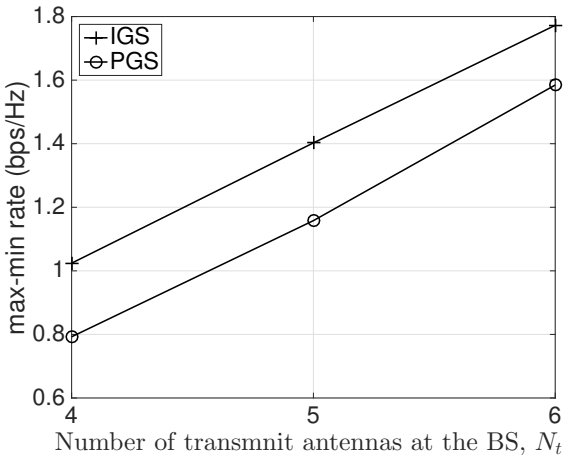

Fig. 3. Optimized max-min user rate versus different number of transmit transmit antennas, N_t, at the BS.

we set the same power budget for each cell, i.e., $P_i \equiv P$, $\forall\, i \in \mathcal{I}$. We set noise power desnity $\frac{\sigma^2}{B} = -174$ dBm/Hz with bandwidth $B = 20$ MHz. To analyze the proposed algorithm through simulations, we assume $K = 6$ users per cell, where each user has $N_r = 2$ receive antennas. Unless stated otherwise, each BS is equipped with $N_t = 4$ antennas and the BS transmit power is set to $P = 26$ dBm.

We compare the performance of the proposed Algorithm 1, which employs IGS, with the conventional PGS Algorithm, which will solve for similar problem (7) with zero pseudo-covariance matrix, i.e., $\widetilde{\mathbf{C}}_{i,j} = \mathbf{0}^{N_t \times N_t}\ \forall\ (i,j) \in \mathcal{I} \times \mathcal{J}$. Alternatively, WMMSE Algorithm [12] is also applicable for designing $\mathbf{F}_{m,k} \in \mathbb{C}^{N_t \times N_t}$ such that $\mathbf{C}_{m,k} = \mathbf{F}_{m,k}\mathbf{F}_{m,k}^H$, which achieves a similar performance to Alg. 1 for PGS in our computational experience. Fig. 2 plots the achievable max-min rate versus the transmit power budget, P, which clearly demonstrates the advantage of using IGS over conventional PGS. As expected the max-min rate increases with the increase of the available power budget, where the performance gap between IGS and PGS is wider with the increase in the available transmit power budget. This might be because of potential

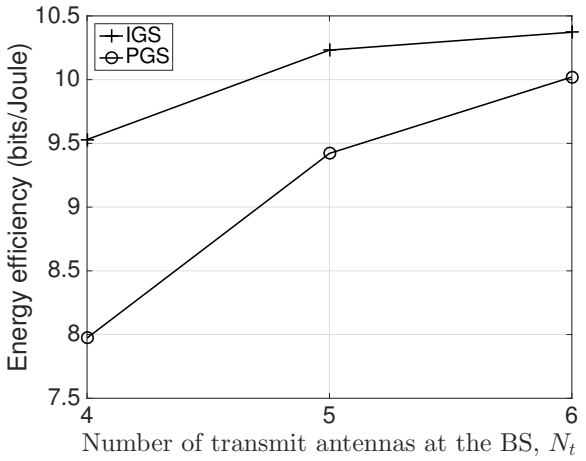

Fig. 4. Optimized energy efficiency versus different number of transmit transmit antennas, N_t, at the BS.

better pseudo-covariance design for IGS in the presence of increased power budget. Fig. 3 plots the achievable max-min rate versus the number of transmit antennas, N_t, at the BS, where the performance gain of IGS over conventional PGS is also seen.

TABLE I
AVERAGE NUMBER OF ITERATIONS REQUIRED BEFORE CONVERGENCE BY THE IGS AND PGS ALGORITHMS FOR $N_t = 4$ ANTENNAS

Algorithm	$P = 20$ dBm	$P = 24$ dBm	$P = 28$ dBm
IGS	17	23.5	32.1
PGS	11.4	13.9	15.6

Due to the additional pseudo-covariance matrices, the computational complexity of the proposed IGS Algorithm 1 is $\mathcal{O}\left((2KNN_t^2)^3\,(KN+N)\right)$ [19] compared to $\mathcal{O}\left((KNN_t^2)^3\,(KN+N)\right)$ of its PGS implementation. The average number of iterations required before convergence for the two algorithms is shown in Table I.

To simulate the energy-efficiency (EE) problem (11), we set $r_{i,j}^{\min} \equiv 0.5$ bps/Hz and set the per antenna circuit power at the BSs, $P_u = 189$ mW [22]. Fig. 4 plots the achievable energy efficiency versus the number of transmit antennas, N_t, at the BS. Again, we can see the sizable performance gain of IGS over conventional PGS. The energy efficiency though increases with the increase in the number of transmit antennas but the increase is not linear. There is marginal increase in the EE for the number of transmit antennas, N_t, increases from 5 to 6 due to increase in the non-transmission power, P_{non}, which is a constant factor, proportional to N_t, in the denominator of EE.

V. CONCLUSIONS

The paper has considered the advantageous IGS for a multi-user multi-cell MIMO network. Accordingly, a path-following algorithm of low computational complexity has been proposed for computation. The numerical examples have supported its practical efficiency, where IGS has been shown clearly outperform PGS in terms of the max-min rate and energy efficiency. Extensions to the case of secure IGS or comparing IGS and PGS in time-sharing context [23] can be considered in future research.

REFERENCES

[1] V. R. Cadambe, S. A. Jafar, and C. Wang, "Interference alignment with asymmetric complex signaling – Settling the Host-Madsen-Nosratinia conjecture," *IEEE Trans. Inf. Theory*, vol. 56, no. 9, pp. 4552–4565, Sept. 2010.

[2] S. A. Jafar, "Interference alignment-a new look at signal dimensions in a communication network," *Found. Trends Commun. Inf. Theory*, vol. 7, no. 1, pp. 1–134, 2011. [Online]. Available: http://dx.doi.org/10.1561/0100000047

[3] S. Lagen, A. Agustin, and J. Vidal, "On the superiority of improper Gaussian signaling in wireless interference MIMO scenarios," *IEEE Trans. Commun.*, vol. 64, no. 8, pp. 3350–3368, Aug. 2016.

[4] Y. Zeng, C. M. Yetis, E. Gunawan, Y. L. Guan, and R. Zhang, "Transmit optimization with improper Gaussian signaling for interference channels," *IEEE Trans. Signal Process.*, vol. 61, no. 11, pp. 2899–2913, Jun. 2013.

[5] C. Hellings and W. Utschick, "Improper signaling versus time-sharing in the SISO Z-interference channel," *IEEE Commun. Lett.*, vol. 21, no. 11, pp. 2432–2435, Nov. 2017.

[6] E. Kurniawan and S. Sun, "Improper Gaussian signaling scheme for the Z-interference channel," *IEEE Trans. Wirel. Commun.*, vol. 14, no. 7, pp. 3912–3923, Jul. 2015.

[7] C. Lameiro, I. Santamaria, and P. J. Schreier, "Rate region boundary of the SISO Z-interference channel with improper signaling," *IEEE Trans. Commun.*, vol. 65, no. 3, pp. 1022–1034, Mar. 2017.

[8] L. Yang and W. Zhang, "Interference alignment with asymmetric complex signaling on MIMO X channels," *IEEE Trans. Commun.*, vol. 62, no. 10, pp. 3560–3570, Oct. 2014.

[9] C. Hellings, M. Joham, and W. Utschick, "QoS feasibility in MIMO broadcast channels with widely linear transceivers," *IEEE Signal Process. Letts.*, vol. 20, no. 11, pp. 1134–1137, Nov. 2013.

[10] S. Lagen, A. Agustin, and J. Vidal, "Coexisting linear and widely linear transceivers in the MIMO interference channel," *IEEE Trans. Signal Process.*, vol. 64, no. 3, pp. 652–664, Feb. 2016.

[11] S. Christensen, R. Agarwal, E. Carvalho, and J. Cioffi, "Weighted sum-rate maximization using weighted MMSE for MIMO-BC beamforming design," *IEEE Trans. Wirel. Commun.*, vol. 7, no. 12, pp. 4792–4799, Dec. 2008.

[12] M. Razaviyayn, M. Hong, and Z.-Q. Luo, "Linear transceiver design for a mimo interfering broadcast channel achieving maxmin fairness," *Signal Processing*, vol. 93, no. 12, pp. 3327 – 3340, 2013.

[13] P. J. Schreier and L. L. Scharf, *Statistical Signal Processing of Complex-Valued Data: The Theory of Improper and Noncircular Signals*. Cambridge Univ. Press, 2010.

[14] I. E. Telatar, "Capacity of multi-antenna Gaussian channels," *Eur. Trans. Telecommun.*, vol. 10, no. 6, pp. 585–595, Nov./Dec. 1999.

[15] H. Tuy, *Convex Analysis and Global Optimization (second edition)*. Springer International, 2016.

[16] H. H. Kha, H. D. Tuan, and H. H. Nguyen, "Fast global optimal power allocation in wireless networks by local D.C. programming," *IEEE Trans. Wirel. Commun.*, vol. 11, no. 2, pp. 510–515, Feb. 2012.

[17] H. D. Tuan, H. H. M. Tam, H. H. Nguyen, T. Q. Duong, and H. V. Poor, "Superposition signaling in broadcast interference networks," *IEEE Trans. Commun.*, vol. 65, no. 11, pp. 4646–4656, Nov. 2017.

[18] U. Rashid, H. D. Tuan, H. H. Kha, and H. H. Nguyen, "Joint optimization of source precoding and relay beamforming in wireless MIMO relay networks," *IEEE Trans. Commun.*, vol. 62, no. 2, pp. 488–499, Feb. 2014.

[19] D. Peaucelle, D. Henrion, and Y. Labit, "Users guide for SeDuMi interface 1.03," 2002. [Online]. Available: http://homepages.laas.fr/peaucell/software/sdmguide.pdf

[20] A. A. Nasir, H. D. Tuan, D. T. Ngo, T. Q. Duong, and H. V. Poor, "Beamforming design for wireless information and power transfer systems: Receive power-splitting vs transmit time-switching," *IEEE Trans. Commun.*, vol. 65, no. 2, pp. 876–889, 2017.

[21] S. Sun, T. S. Rappaport, S. Rangan, T. A. Thomas, A. Ghosh, I. Z. Kovacs, I. Rodriguez, O. Koymen, A. Partyka, and J. Jarvelainen, "Propagation path loss models for 5G urban micro- and macro-cellular scenarios," in *Proc. IEEE Veh. Tech. Conf. (VTC Spring)*, May 2016, pp. 1–6.

[22] C. Xiong, G. Y. Li, S. Zhang, Y. Chen, and S. Xu, "Energy-efficient resource allocation in OFDMA networks," *IEEE Trans. Commun.*, vol. 60, no. 12, pp. 3767–3778, Dec. 2012.

[23] C. Hellings and W. Utschick, "Improper signaling versus time-sharing in the two-user Gaussian interference channel with TIN," *ArXiv Technical Report*, 2018. [Online]. Available: https://arxiv.org/pdf/1808.01611.pdf